

Synthesis, characterization and thermal decomposition of 2'-amino-6'-(1*H*-indol-3-yl)-1-methyl-2-oxospiro-[indoline-3,4'-pyran]-3',5'-dicarbonitrile under non-isothermal condition in nitrogen atmosphere

Ganesan Nalini ¹, Natesan Jayachandramani ¹, Radhakrishnan Suresh ², Venugopal Thanikachalam ^{3,*} and Govindasamy Manikandan ³

¹ Department of Chemistry, Pachaiyappa's College, Chennai, 600030, India

² Department of Chemistry, Presidency College, Chennai, 600005, India

³ Department of Chemistry, Annamalai University, Annamalaiagar, 608002, India

* Corresponding author at: Department of Chemistry, Annamalai University, Annamalaiagar, 608002, India.

Tel.: +91.4144.239523. Fax: +91.4144.238080. E-mail address: profvt.chemau@gmail.com (V. Thanikachalam).

ARTICLE INFORMATION



DOI: 10.5155/eurjchem.7.3.380-386.1442

Received: 24 April 2016

Accepted: 21 May 2016

Published online: 30 September 2016

Printed: 30 September 2016

KEYWORDS

Spirooxindole
 Coats-Redfern method
 Thermal decomposition
 Flynn-Wall-Ozawa method
 Thermodynamic parameters
 Kissinger-Akahira-Sunose method

ABSTRACT

The kinetics and decomposition of a new spirooxindole compound, 2'-amino-6'-(1*H*-indol-3-yl)-1-methyl-2-oxospiro[indoline-3,4'-pyran]-3',5'-dicarbonitrile was studied by thermo gravimetric technique under non-isothermal conditions. The kinetic parameters were calculated using model-free (Friedman, Kissinger-Akahira-Sunose and Flynn-Wall-Ozawa methods) and model-fitting (Coats-Redfern) methods. The results of the Friedman isoconversional analysis of the thermogravimetric data suggested that the investigated decomposition process follows a single-step.

Cite this: *Eur. J. Chem.* 2016, 7(3), 380-386

1. Introduction

Synthetic or natural heterocyclic compounds containing spirooxindole framework are endowed with a wide range of pharmacological activities [1]. The 3-substituted indole nucleus substructure is one of the most important heterocyclic found in natural products, pharmaceutical and medicinal chemistry [2]. The heterocyclic spirooxindoles are attractive targets of medicinal chemistry due to the wide range of pharmacological activities such as anticancer, anti-microbial, anti-malarial, anti-mycobacterium, anti-oxidant and anti-fungal activities [3]. Catalytic stereo-selective synthesis of diverse oxindoles and spirooxindoles were obtained from isatins [4]. Their preparative methods suffer from tedious synthetic routes, longer reaction time, drastic reaction conditions, as well as narrow substrate scope [5]. Spirocyclic oxindoles have been generated containing a six-membered spiro cyclic moiety, especially a six membered piperidine structure. These compounds have a broad spectrum of biological activities, non-peptidyl growth hormone secretagogues and potent non-

peptide inhibitors that may have utility as anti-cancer agents [6]. An effective reflexive-Michael reaction has been disclosed to access drug-like six-membered spirooxindoles in good yields and excellent antio-selectivities by using amino enzyme-catalysis [7]. Novel dispirooxindole-pyrrolidine derivatives have been synthesized through 1,3-dipolar cycloaddition of an azomethine ylide generated from isatin and sarco-sine with the dipolarophile 3-(1*H*-indole-3-yl)-3-oxo-2-(2-oxo indolin-3-ylidene)propanenitrile and also spiro compound of acenaphthenequinone obtained by the same optimized reaction condition. The synthesized compounds were evaluated for their antimicrobial activity and all the compounds showed significant activity [8]. Recent advances in the synthesis of biologically active spirooxindoles with potential use as therapeutic agents were reported [9]. The search for novel anti-cancer agents with more selectivity and lower toxicity continues to be an area of intense investigation. The unique structural features of spirooxindoles together with diverse biological activities have made them privileged structures in new drug discovery [10]. Non-isothermal decomposition

kinetics of chitosan [11], chitin [12], cephalosporins [13], procaine and benzocaine [14], theobromine [15] and spirooxindole [16] were studied in detail and appropriate kinetic models were proposed. 3-Chloro oxindoles are versatile starting materials for asymmetric organo catalytic synthesis of spirooxindoles.

Literature data show that no work has been reported on thermal decomposition of spirooxindoles by one-pot multicomponent system at different heating rates (10, 15, 20 and 30 K/min) under non-isothermal condition in nitrogen atmosphere. In this paper, we report the synthesis and thermal decomposition of 2'-amino-6'-(1H-indol-3-yl)-1-methyl-2-oxospiro[indoline-3, 4'-pyran]-3', 5'-dicarbonitrile (Figure 1) [17] and its thermal decomposition under non-isothermal dynamic nitrogen atmospheric condition. The kinetic and thermodynamic parameters were calculated by using model-fitting and model free-methods.

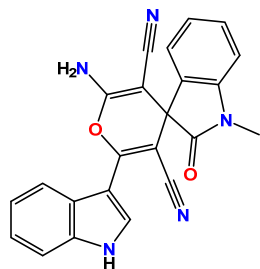


Figure 1. Structure of AIMOIPD.

2. Experimental

2.1. Preparation of 2'-amino-6'-(1H-indol-3-yl)-1-methyl-2-oxospiro[indoline-3,4'-pyran]-3',5'-dicarbonitrile (AIMOIPD)

To a stirred solution of *N*-methyl isatin (0.147 g, 1 mmol), ethylcyano acetate (0.066 g, 1 mmol), 3-cyanoacetyl indole (0.184 g, 1 mmol) in methanol (10 mL) and triethylamine (20 mol %) were added and stirring was continued for 30 min. On completion, the reaction mixture was poured into crushed ice and the precipitate formed was filtered, dried and purified by column chromatography to afford the pure product. The isolated product was further purified by recrystallization in ethanol and the appropriate yield of the product was 89%. Color: Pale brown solid. M.p.: 205-208 °C. *R_f*: 0.27 (40%, AcOEt:Petroleum ether). FT-IR (KBr, ν , cm^{-1}): 1152, 1250, 1356, 1416, 1471, 1526, 1617, 1666, 2202, 2368, 2929, 3171, 3360. ^1H NMR (500 MHz, DMSO- d_6 , δ , ppm): 3.19 (s, 3H, N-CH₃), 7.12-7.18 (m, 3H, Ar-H), 7.23 (t, J = 6.85 Hz, 1H, Ar-H), 7.38-7.42 (m, 2H, Ar-H), 7.49 (d, J = 8.4 Hz, 1H, Ar-H), 7.65 (s, 2H, -NH₂), 7.96 (d, J = 8.45 Hz, 1H, Ar-H), 8.15 (d, J = 3.05 Hz, 1H, Ar-H), 12.06 (brs, 1H, NH). ^{13}C NMR (125 MHz, DMSO- d_6 , δ , ppm): 27.1, 50.1, 54.4, 81.4, 105.5, 109.7, 113.0, 117.5, 117.8, 121.8, 122.1, 123.4, 124.2, 124.9, 125.4, 130.6, 131.5, 136.5, 143.5, 158.5, 160.3, 176.0. MS (EI, m/z): 394.00 [M⁺+H⁺]. Anal. calcd. for C₂₃H₁₅N₅O₂: C, 70.22; H, 3.84; N, 17.80. Found: C, 70.31; H, 3.85; N, 17.92%.

2.2. Instrumentation

Elemental analysis was performed at Central Leather Research Institute (CLRI), Chennai, India. IR measurements were done as KBr pellets for solids using Perkin Elmer Spectrometer RXI FT-IR. The ^1H and ^{13}C NMR spectra were recorded in DMSO- d_6 , using TMS as internal standard with JEOL ECA-500MHz high resolution NMR spectrometer. The mass spectrum was recorded using an Electrospray Ionization Method with ThermoFinnigan mass spectrometer. Melting

point was determined in capillary tubes and is uncorrected. Analytical TLC was performed on pre-coated plastic sheets of silica gel G/UV-254 of 0.2mm thickness. The simultaneous TGA curves were obtained with the thermal analysis system model Perkin Elmer TAC7/DX (Thermal Analysis Controller TAC-7). The TG/DTG analyzes of AIMOIPD were carried out under dynamic nitrogen atmosphere (100 mL/min) in an iron pan with the sample at the heating rates 10, 15, 20 and 30 K/min from 30 to 1150°C. TG/DTG was recorded at Indian Institute of Technology, Chennai, India. The kinetic parameters E_a and A were calculated using Microsoft Excel Software. The sample temperature which was controlled by a thermocouple, did not exhibit any systematic deviation from the preset linear temperature program.

2.3. Theoretical background

2.3.1. Model fitting method

For non-isothermal experiment, model fitting involves different models to α - temperature (α -T) curves and successfully determine E_a and A . There are numerous non-isothermal model fitting methods and the most popular one is the Coats and Redfern method [18]. This method has been most successfully used for studying the kinetics of dehydration and vaporization of different solid substances [19]. The kinetic parameters can be derived from modified Coats and Redfern Equation (1),

$$\ln \left[\frac{g(\alpha)}{T^2} \right] = \ln \left[\frac{AR}{\beta E_a} \left[1 - \left(\frac{2RT^*}{E_a} \right) \right] \right] - \frac{E_a}{RT} \quad (1)$$

where $g(\alpha)$ is an integral form of the conversion function (α), the expression of which depends on the kinetic model of the occurring reaction. If the correct $g(\alpha)$ function is used, a plot of $\ln[g(\alpha)/T^2]$ against $1/T$ should give a straight line from which the values of the activation energy, E_a and the pre-exponential factor, A can be calculated.

2.3.2. Model free methods

Friedman method [20] is a differential method and is one of the first used iso-conversional methods. This model according to logarithmic form of Equation (3).

$$\frac{d\alpha}{dt} = A \exp \left(\frac{-E_a}{RT} \right) f(\alpha) \quad (2)$$

gives

$$\ln \left[\beta \frac{d\alpha}{dT} \right] = \ln [A \cdot f(\alpha)] - \frac{E_{a,\alpha}}{RT_{\alpha}} \quad (3)$$

The plots of $\ln(\beta \cdot d\alpha/dT)$ vs $1/T$ (Equation (3)), at each α value were drawn and from the slope of the plots, we can calculate E_a values.

The isoconversional integral method suggested independently by Flynn and Wall [21] and Ozawa [22], and is based on the Equation (4),

$$\ln \beta = \ln \left[\frac{0.0048 \cdot A \cdot E_a}{g(\alpha) \cdot R} \right] - 1.0516 \frac{E_a}{RT} \quad (4)$$

and for Kissinger-Akahira-Sunose (KAS) method [23,24], Equation (5) is used.

$$\ln(\beta/T^2) = \ln \left[\frac{A E_a}{g(\alpha) R} \right] - \frac{E_a}{RT} \quad (5)$$

The plots of $\ln(\beta d\alpha/dT)$ vs $1/T$ (Equation (3)), $\ln\beta$ vs $1/T$ (Equation (4)) and $\ln(\beta/T^2)$ vs $1/T$ (Equation (5)) have been shown to give the values of apparent activation energies for the decomposition of AIMOIPD at different values of α . According to these equations, the reaction mechanism and shape of $g(\alpha)$ function do not affect the values of the activation energies of the decomposition stages.

2.3.3. Thermodynamic parameters

The kinetic parameters, energy of activation (E_a) and pre-exponential factor (A) obtained from Kissinger single point [23] kinetic method uses the Equation (6):

$$\ln \left(\frac{\beta}{T_m^2} \right) = - \frac{E_a}{RT_m} + \ln \left(\frac{AR}{E_a} \right) \quad (6)$$

where T_m is the temperature that corresponds to the maximum of $d\alpha/dT$. This model-free kinetic method can be applied with a reasonable approximation without being limited to n-order kinetics [25], by providing a single E_a value for each reaction step.

Based on the values of activation energy and pre-exponential factor for the decomposition stage, the values of ΔS^\ddagger , ΔH^\ddagger and ΔG^\ddagger for the formation of activated complex from the reactant were calculated [25-27].

3. Results and discussion

3.1. Non-isothermal TGA

The TGA method of thermograms of pure AIMOIPD recorded in a dynamic nitrogen atmosphere at different heating rates of 10, 15, 20 and 30 K/min are represented in Figure 2. The thermal decomposition process of AIMOIPD was observed in three stages. The thermogravimetric curves showed that the first stage decomposition starts at 150 °C and ends at about 275 °C with the corresponding mass loss of 28.46%. The second-stage decomposition starts at 275 °C and ends at about 550 °C with the corresponding mass loss of 41.26%. The third stage starts at 550 °C and ends at about 840 °C with the corresponding mass loss of 9.41%.

3.2. Model-free analysis

The non-isothermal decomposition kinetics of AIMOIPD was first analyzed by model-free methods viz., Friedmann, Kissinger-Akahira-Sunose and Flynn-Wall-Ozawa. The data showed the decomposition of apparent activation energy E_a , as a function of extent of conversion α for the decomposition of AIMOIPD. At all the stages, E_a value increases slightly in the conversion range of $0.12 \leq \alpha \leq 0.98$. It was pointed out [28] that when E_a changes with α , the Friedmann and KAS isoconversional methods led to close values of E_a for all the stages. The applied isoconversional method does not suggest a direct way for evaluating either the pre-exponential factor or the analytical form of the reaction model $f(\alpha)$ for the investigated decomposition process of AIMOIPD.

In the first stage decomposition of AIMOIPD, the values of E_a corresponding to the values of α for the decomposition process obtained by Friedmann, KAS and FWO methods are given in Figure 3. It is seen that E_a value depends upon the extent of conversion (α). The average values of E_a in the range $0.12 \leq \alpha \leq 0.98$ is 230.57 ± 0.52 kJ/mol in Friedman method. From Figure 3, it is evident that the values of activation energy obtained by KAS and FWO methods are $E_a = 229.76 \pm 0.43$

kJ/mol, KAS; 226.45 ± 0.42 kJ/mol, FWO. The apparent activation energy initially decreases slightly with increase in the degree of conversion $0.12 \leq \alpha \leq 0.30$ and then remains constant which indicates slower rate of decomposition and the gaseous products are not in equilibrium with the solid compound.

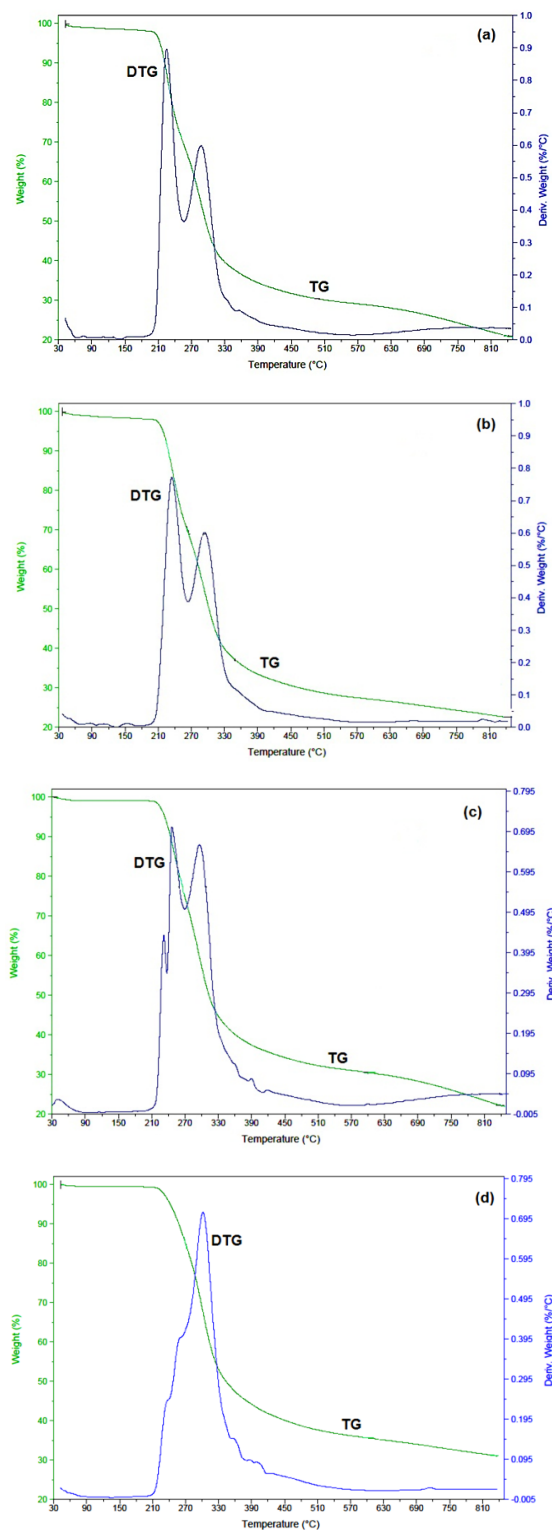


Figure 2. TG and DTA curves of AIMOIPD at heating rates of (a) 10 K/min, (b) 15 K/min, (c) 20 K/min and (d) 30 K/min in nitrogen atmosphere.

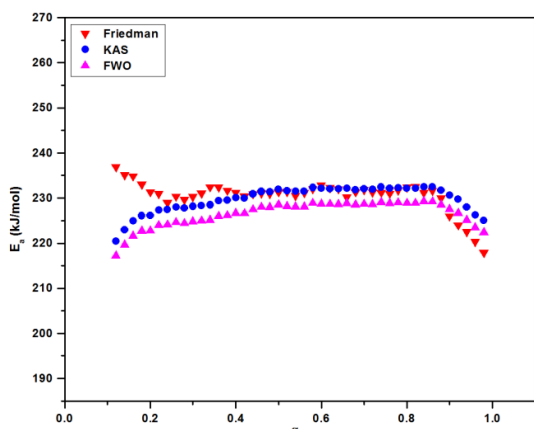


Figure 3. E_a versus α plot for the decomposition of AIMOIPD under non-isothermal condition (Stage I).

For stage II, the variation of E_a with α for the decomposition is shown in Figure 4. The average value of E_a is 231.70 ± 0.51 kJ/mol (KAS method). It is evident that the KAS method of activation energy is higher than the values of activation energy obtained by Friedmann ($E_a = 228.68 \pm 0.41$ kJ/mol) and FWO ($E_a = 229.63 \pm 0.42$ kJ/mol) methods.

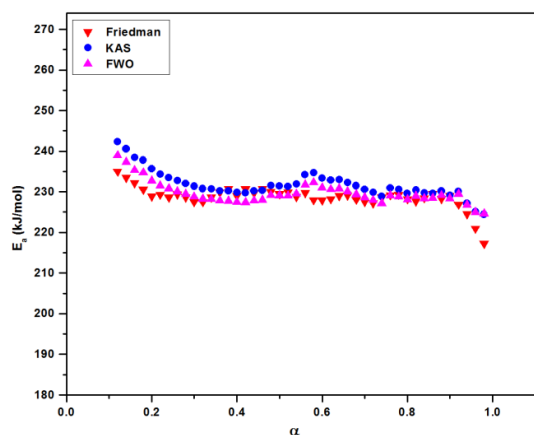


Figure 4. E_a versus α plot for the decomposition of AIMOIPD under non-isothermal condition (Stage II).

For stage III, the values of apparent activation energies obtained by Friedman and KAS methods are higher than that of FWO method. The average values of E_a in the range $0.12 \leq \alpha \leq 0.98$ are 537.95 ± 0.62 kJ/mol (Friedman), 535.21 ± 1.72 kJ/mol (KAS) and 524.74 ± 1.74 kJ/mol (FWO) (Figure 5) from the average values of E_a for each stage, the rate of decomposition is found to depend upon the nature of the intermediate formed during the decomposition and the third stage is slower than the other stages. The higher values activation energy for stage III than the other stages indicates that the intermediate compounds are thermally more stable and the decomposition process is slow.

3.3. Model-fitting analysis

After carrying out model free analysis, model fitting can be done in the conversion region where apparent activation energy is approximately constant where a single model may fit. The non-isothermal kinetic data of AIMOIPD at $0.12 \leq \alpha \leq 0.98$ where model free analysis indicated approximately constant activation energy, were then fitted to each of the 15 models listed in the Tables 1-3 for stages I, II and III,

respectively. The values of Arrhenius parameters were computed by applying Coats-Redfern method. It is found that these parameters are highly variable, exhibiting strong dependence on the reaction model chosen. The decomposition stages are also confirmed by invariant kinetic parameters method.

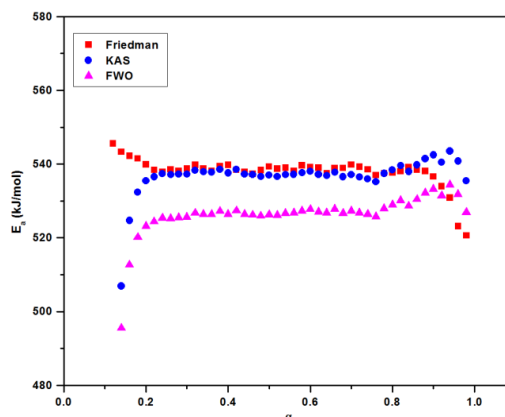


Figure 5. E_a versus α plot for the decomposition of AIMOIPD under non-isothermal condition (Stage III).

3.4. Invariant kinetic parameters (IKP) analysis

The invariant kinetic parameters were calculated for the heating rates of 10, 15, 20 and 30 K/min using Coats-Redfern method, in the range $0.12 \leq \alpha \leq 0.98$ for AIMOIPD, the straight lines corresponding to Coats-Redfern method is characterized by correlation coefficient values close to unity.

For several groups of apparent activation parameters, obtained by different kinetic models, we tried to establish the best combination ($r \rightarrow 1$), a better resolution in determining the Invariant kinetic parameters and closet value to the mean isoconversional activation energies [29-31].

In stage I for AKM-{A2}, the plot of $\ln A$ vs E_a has the highest correlation coefficient and is a straight line (Figure 6). The invariant kinetic parameters, $E_{inv} = 231.89$ kJ/mol and $\ln A_{inv} = 53.70$ are obtained with $r = 0.997$ (Figure 6). For these group, the invariant activation energy is almost equal $E_a = 231.89$ kJ/mol compared to Friedman, KAS and FWO methods (230.57 ± 0.52 kJ/mol, Friedmann; 229.76 ± 0.43 kJ/mol, KAS; 226.45 ± 0.42 kJ/mol, FWO).

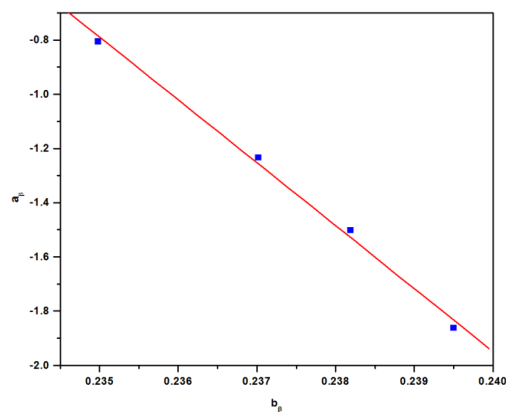


Figure 6. Supercorrelation (Compensation effect parameters) plot for the best combination of kinetic models (Stage I).

For stage II, a better resolution in determining the invariant kinetic parameters and the correlation coefficients (Figure 7) show a good agreement of all kinetic models.

Table 1. Arrhenius parameters for non-isothermal decomposition of AIMOIPD (Stage I) at various heating rates.

| Kinetic model | $\beta = 10 \text{ K/min}$ | | | $\beta = 15 \text{ K/min}$ | | | $\beta = 20 \text{ K/min}$ | | | $\beta = 30 \text{ K/min}$ | | |
|---------------|----------------------------|---------|--------|----------------------------|---------|--------|----------------------------|---------|--------|----------------------------|---------|--------|
| | E_a (kJ/mol) | $\ln A$ | r |
| P2 | 48.07 | 9.73 | -0.969 | 46.60 | 9.68 | -0.971 | 46.15 | 9.79 | -0.969 | 47.95 | 10.54 | -0.969 |
| P3 | 29.23 | 4.82 | -0.963 | 28.23 | 4.91 | -0.966 | 27.92 | 5.07 | -0.963 | 29.09 | 5.72 | -0.962 |
| P4 | 19.86 | 2.25 | -0.955 | 19.11 | 2.40 | -0.958 | 18.86 | 2.58 | -0.955 | 19.72 | 3.18 | -0.954 |
| F1 | 166.06 | 39.38 | -0.996 | 161.42 | 38.41 | -0.997 | 160.28 | 38.22 | -0.997 | 166.04 | 39.68 | -0.996 |
| F2 | 253.91 | 61.41 | -0.999 | 246.67 | 59.71 | -0.999 | 245.18 | 59.34 | -0.999 | 253.97 | 61.33 | -0.999 |
| F3 | 364.11 | 88.83 | -0.993 | 353.56 | 86.19 | -0.992 | 351.67 | 85.60 | -0.993 | 364.27 | 88.27 | -0.993 |
| D1 | 230.22 | 61.36 | -0.977 | 224.37 | 60.04 | -0.979 | 222.70 | 59.66 | -0.978 | 230.35 | 61.44 | -0.977 |
| D2 | 250.50 | 58.52 | -0.984 | 243.85 | 56.96 | -0.986 | 242.01 | 56.51 | -0.985 | 250.54 | 58.45 | -0.984 |
| D3 | 293.68 | 67.82 | -0.992 | 285.79 | 65.92 | -0.993 | 283.76 | 65.37 | -0.992 | 293.76 | 67.57 | -0.992 |
| D4 | 264.70 | 60.57 | -0.987 | 257.64 | 58.90 | -0.989 | 255.74 | 58.42 | -0.988 | 264.75 | 60.44 | -0.987 |
| A2 | 78.86 | 17.83 | -0.996 | 76.52 | 17.53 | -0.997 | 75.93 | 17.57 | -0.996 | 78.77 | 18.51 | -0.996 |
| A3 | 49.74 | 10.42 | -0.995 | 48.16 | 10.34 | -0.996 | 47.75 | 10.46 | -0.996 | 49.62 | 11.22 | -0.995 |
| A4 | 35.26 | 6.62 | -0.994 | 34.07 | 6.65 | -0.996 | 33.75 | 6.80 | -0.995 | 35.14 | 7.49 | -0.995 |
| R2 | 132.06 | 30.07 | -0.988 | 128.39 | 29.38 | -0.990 | 127.40 | 29.27 | -0.988 | 132.01 | 30.52 | -0.988 |
| R3 | 122.56 | 27.93 | -0.984 | 119.16 | 27.32 | -0.986 | 118.22 | 27.23 | -0.984 | 122.50 | 28.42 | -0.984 |

Table 2. Arrhenius parameters for non-isothermal decomposition of AIMOIPD (Stage II) at various heating rates.

| Kinetic model | $\beta = 10 \text{ K/min}$ | | | $\beta = 15 \text{ K/min}$ | | | $\beta = 20 \text{ K/min}$ | | | $\beta = 30 \text{ K/min}$ | | |
|---------------|----------------------------|---------|--------|----------------------------|---------|--------|----------------------------|---------|--------|----------------------------|---------|--------|
| | E_a (kJ/mol) | $\ln A$ | r |
| P2 | 9.21 | -1.82 | -0.659 | 8.797 | -1.575 | -0.654 | 8.53 | -1.40 | -0.648 | 8.96 | -0.89 | -0.652 |
| P3 | 2.85 | -4.21 | -0.373 | 2.553 | -3.993 | -0.349 | 2.35 | -3.84 | -0.328 | 2.61 | -3.31 | -0.348 |
| P4 | -0.31 | - | 0.058 | -0.550 | - | 0.105 | -0.72 | - | 0.138 | -0.55 | - | 0.102 |
| F1 | 51.49 | 8.79 | -0.909 | 50.232 | 8.832 | -0.912 | 49.50 | 8.88 | -0.912 | 51.11 | 9.53 | -0.910 |
| F2 | 85.47 | 16.90 | -0.960 | 83.480 | 16.747 | -0.962 | 82.37 | 16.69 | -0.963 | 84.97 | 17.47 | -0.961 |
| F3 | 128.48 | 26.88 | -0.981 | 125.548 | 26.476 | -0.982 | 123.97 | 26.27 | -0.983 | 127.82 | 27.22 | -0.981 |
| D1 | 76.65 | 20.93 | -0.876 | 75.164 | 20.909 | -0.879 | 74.30 | 20.92 | -0.880 | 76.45 | 21.64 | -0.878 |
| D2 | 78.66 | 13.34 | -0.875 | 76.924 | 13.246 | -0.877 | 75.89 | 13.21 | -0.878 | 78.25 | 13.95 | -0.876 |
| D3 | 94.99 | 15.71 | -0.902 | 92.915 | 15.530 | -0.905 | 91.70 | 15.44 | -0.905 | 94.52 | 16.24 | -0.903 |
| D4 | 84.02 | 13.11 | -0.885 | 82.173 | 12.992 | -0.888 | 81.08 | 12.94 | -0.888 | 83.59 | 13.70 | -0.886 |
| A2 | 20.82 | 1.62 | -0.868 | 20.168 | 1.820 | -0.870 | 19.77 | 1.97 | -0.868 | 20.53 | 2.51 | -0.867 |
| A3 | 10.58 | -1.15 | -0.797 | 10.126 | -0.906 | -0.796 | 9.84 | -0.73 | -0.791 | 10.31 | -0.22 | -0.792 |
| A4 | 5.49 | -2.84 | -0.670 | 5.136 | -2.597 | -0.660 | 4.91 | -2.42 | -0.648 | 5.24 | -1.91 | -0.656 |
| R2 | 38.56 | 4.89 | -0.865 | 37.580 | 5.005 | -0.867 | 36.99 | 5.10 | -0.867 | 38.23 | 5.70 | -0.865 |
| R3 | 35.00 | 4.26 | -0.848 | 34.085 | 4.395 | -0.850 | 33.53 | 4.50 | -0.850 | 34.68 | 5.09 | -0.848 |

Table 3. Arrhenius parameters for non-isothermal decomposition of AIMOIPD (Stage III) at various heating rates.

| Kinetic model | $\beta = 10 \text{ K/min}$ | | | $\beta = 15 \text{ K/min}$ | | | $\beta = 20 \text{ K/min}$ | | | $\beta = 30 \text{ K/min}$ | | |
|---------------|----------------------------|---------|--------|----------------------------|---------|--------|----------------------------|---------|--------|----------------------------|---------|--------|
| | E_a (kJ/mol) | $\ln A$ | r |
| P2 | 13.29 | -2.87 | -0.985 | 13.40 | -2.45 | -0.985 | 13.50 | -2.16 | -0.985 | 13.12 | -1.86 | -0.985 |
| P3 | 3.36 | -5.33 | -0.894 | 3.42 | -4.91 | -0.894 | 3.46 | -4.61 | -0.893 | 3.17 | -4.35 | -0.881 |
| P4 | -1.57 | - | 0.750 | -1.54 | - | 0.740 | -1.53 | - | 0.731 | -1.78 | - | 0.787 |
| F1 | 73.60 | 6.21 | -0.996 | 74.09 | 6.63 | -0.997 | 74.54 | 6.94 | -0.997 | 73.64 | 7.14 | -0.996 |
| F2 | 116.61 | 12.38 | -0.978 | 117.39 | 12.82 | -0.978 | 118.10 | 13.14 | -0.978 | 116.79 | 13.24 | -0.978 |
| F3 | 170.28 | 19.84 | -0.959 | 171.42 | 20.30 | -0.960 | 172.47 | 20.63 | -0.960 | 170.64 | 20.63 | -0.959 |
| D1 | 119.31 | 19.64 | -0.998 | 120.04 | 20.08 | -0.998 | 120.71 | 20.40 | -0.998 | 119.68 | 20.55 | -0.998 |
| D2 | 119.09 | 10.64 | -1.000 | 119.85 | 11.08 | -1.000 | 120.56 | 11.39 | -1.000 | 119.29 | 11.50 | -1.000 |
| D3 | 140.51 | 12.17 | -1.000 | 141.41 | 12.62 | -1.000 | 142.24 | 12.94 | -1.000 | 140.78 | 13.00 | -1.000 |
| D4 | 126.15 | 10.14 | -1.000 | 126.95 | 10.58 | -1.000 | 127.70 | 10.90 | -1.000 | 126.36 | 10.99 | -1.000 |
| A2 | 28.59 | -0.04 | -0.995 | 28.80 | 0.37 | -0.995 | 28.99 | 0.67 | -0.995 | 28.47 | 0.95 | -0.995 |
| A3 | 13.55 | -2.56 | -0.991 | 13.67 | -2.15 | -0.992 | 13.78 | -1.85 | -0.992 | 13.39 | -1.55 | -0.991 |
| A4 | 6.08 | -4.24 | -0.980 | 6.16 | -3.83 | -0.981 | 6.22 | -3.53 | -0.982 | 5.89 | -3.24 | -0.979 |
| R2 | 56.78 | 3.00 | -1.000 | 57.16 | 3.42 | -1.000 | 57.51 | 3.73 | -1.000 | 56.76 | 3.96 | -1.000 |
| R3 | 52.05 | 2.55 | -1.000 | 52.40 | 2.98 | -1.000 | 52.72 | 3.28 | -0.999 | 52.02 | 3.52 | -1.000 |

The efficiency of IKP method is strongly revealed by AKM- {A2} (Figure 7) and even by AKM all kinetics models which comprise all the best-fitting function that makes it a more powerful method. The invariant activation energy $E_a = 232.46$ kJ/mol is close to KAS method. The invariant kinetic parameters are $E_{inv} = 232.46$ kJ/mol and $\ln A_{inv} = 46.11$ obtained with $r = 0.983$.

In third stage for AKM- {F3} the plots of $\ln A$ vs E_a has the highest correlation ($r = 0.999$) (Figure 8). Depending on the choice of kinetic models, the compensation effect parameters are obtained with different accuracies, their values and the derived invariant activation parameters varying substantially. For AKM- {F3}, the invariant kinetic parameters are 540.56 kJ/mol and $\ln A_{inv} = 74.40$ obtained with $r = 0.999$. For these groups, the invariant activation energy is slightly above 6 units ($E_a = 537.95 \pm 0.62$ kJ/mol) and 14 units below ($E_a = 524.74$ kJ/mol) that obtained by Friedman and FWO methods.

3.5. Determination of kinetic models

The most probable kinetic model for the first stage decomposition process of AIMOIPD is F2. By introducing the derived reaction $g(\alpha) = [(1-\alpha)^{-1}-1]$ the following equation is obtained.

$$[(1-\alpha)^{-1}-1] = \frac{A \cdot E_a}{R \cdot \beta} p(x) \quad (7)$$

The plots of $[(1-\alpha)^{-1}-1]$ against $E_a p(x)/R\beta$ at the different heating rates are shown in Figure 9. By using Equation (7), the values of A was determined from the slope of the line shown in Figure 9. By applying second-order F2 model $E_a = 230.57 \pm 0.52$ kJ/mol, the pre-exponential (frequency) factor $A = 2.097 \times 10^{23}/\text{min}$ ($\ln A = 53.70$). The obtained value of $\ln A$ is in good agreement with values obtained by Friedman iso-conversional intercept.

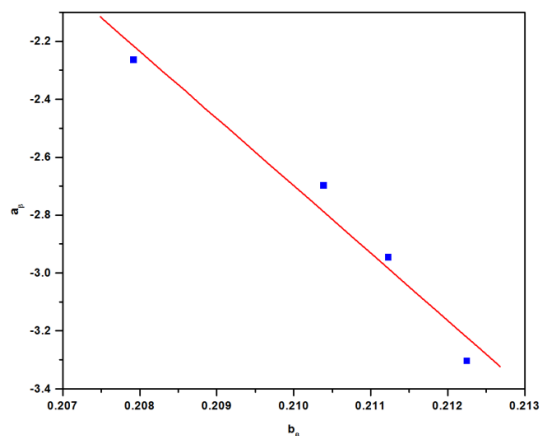


Figure 7. Supercorrelation (Compensation effect parameters) plot for the best combination of kinetic models (Stage II).

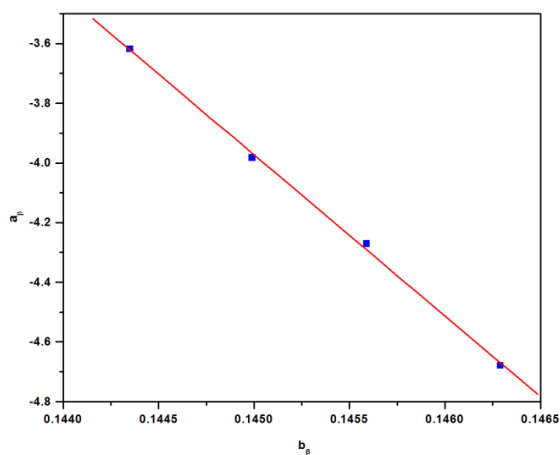


Figure 8. Supercorrelation (Compensation effect parameters) plot for the best combination of kinetic models (Stage III).

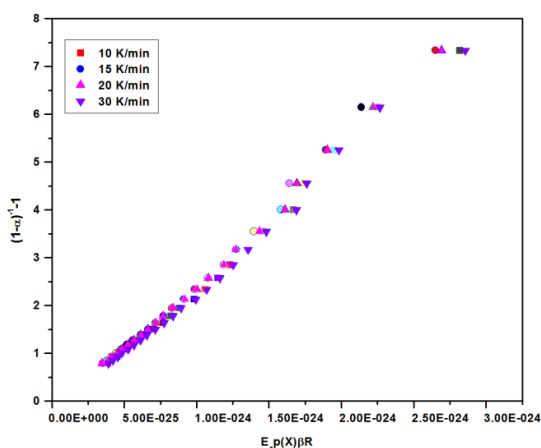


Figure 9. Determination of A value by plotting $(1-\alpha)^{-1}-1$ against $E_a p(x)/\beta R$ for the decomposition process of AIMOIPD at the different heating rates (β) (Stage I).

The most suitable kinetic model for stages II and III is F3 (third-order). By introducing the derived reaction model $g(\alpha)=0.5 [(1-\alpha)^{-2}-1]$, the following equation is obtained.

$$0.5[(1-\alpha)^{-2}-1]=\frac{A.E_a}{R.\beta}p(x) \tag{8}$$

The plots of $0.5[(1-\alpha)^{-2}-1]$ against $E_a p(x)/R.\beta$ at the different (Figures 10 and 11) heating rates are considered. By using Equation (8), the values were calculated from the slopes of the line shown in Figures 10 and 11. By applying the third-order model F3, $E_a = 228.68 \pm 0.41$ kJ/mol; $E_a = 537.95 \pm 0.62$ kJ/mol, stages II and III, respectively, the pre-exponential (frequency) factor $A = 1.060 \times 10^{20}$ /min ($\ln A = 46.11$) and $A = 2.048 \times 10^{32}$ /min ($\ln A = 74.40$) for stages II and III, respectively. The corresponding kinetic equations for describing the non-isothermal decomposition process of AIMOIPD in stages I, II and III are given by

For stage I

$$\beta d\alpha/dT = 2.097 \times 10^{23} \times \exp(-230.57/RT) [(1-\alpha)^2] \tag{9}$$

For stage II

$$\beta d\alpha/dT = 1.060 \times 10^{20} \times \exp(-228.68/RT) [(1-\alpha)^3] \tag{10}$$

For stage III

$$\beta d\alpha/dT = 2.048 \times 10^{32} \times \exp(-537.95/RT) [(1-\alpha)^3] \tag{11}$$

where $(1-\alpha)^2$, $(1-\alpha)^3$ represent the differential form of F₂ (second-order), F₃ (third-order) reaction model for stages I and II, III, respectively.

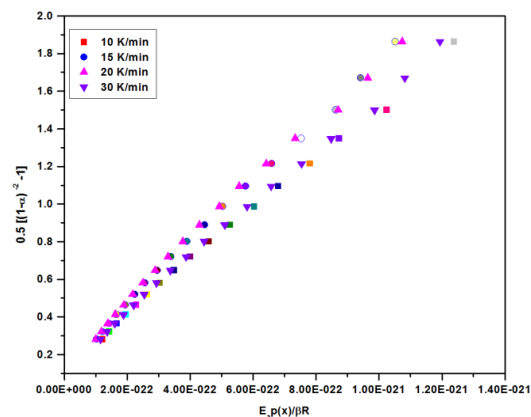


Figure 10. Determination of A value by plotting $0.5[(1-\alpha)^{-2}-1]$ against $E_a p(x)/\beta R$ for the decomposition process of AIMOIPD at the different heating rates (β) (Stage II).

3.6. Thermodynamic parameters

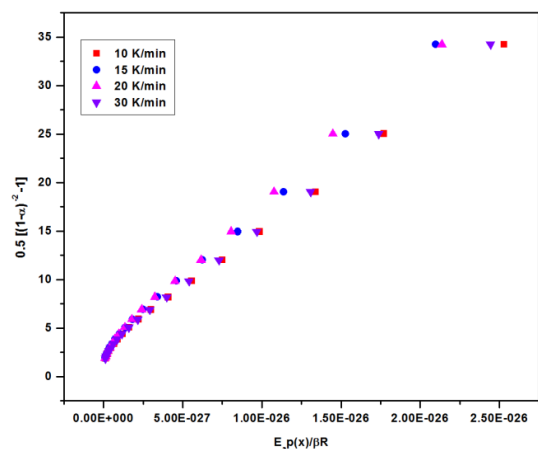
From the DTG curves, the peak temperatures for AIMOIPD are 491.09, 494.32, 496.35 and 498.52 K for stage I and 593.18, 596.95, 597.51 and 598.01 K for stage II and 891.73, 895.00, 897.49 and 898.82 K for stage III. These peak temperatures are used to determine the single point kinetic parameters [23]. The calculated E_a values are 194.14, 414.20, 673.22 kJ/mol for stages I, II and III, respectively.

The thermodynamic parameters ΔS^\ddagger , ΔH^\ddagger and ΔG^\ddagger were calculated at the peak temperatures in reference [32] TG and DTG curve for the corresponding stages [33]. Since the temperature characterizes the higher rate of decomposition, it is an important parameter.

As can be seen from the Table 4, the value of ΔS^\ddagger for all the stages are positive. It means that the corresponding activated complexes were with lower degree of arrangement than the initial state. The positive values of ΔH^\ddagger and ΔG^\ddagger for all the stages show that they are connected with absorption of heat and they represent non-spontaneous processes at normal temperature.

Table 4. Values of kinetic and thermodynamic parameters for the thermal decomposition of AIMOIPD in nitrogen atmosphere.

| Parameter | Stage I | Stage II | Stage III |
|-------------------------------|---------|----------|-----------|
| E_a (kJ/mol) | 194.14 | 414.20 | 673.22 |
| $\ln A$ | 47.46 | 84.12 | 90.64 |
| ΔG^\ddagger (kJ/mol) | 122.20 | 146.35 | 226.12 |
| ΔH^\ddagger (kJ/mol) | 190.03 | 409.24 | 665.78 |
| ΔS^\ddagger (J/K.mol) | 137.22 | 440.39 | 491.23 |
| r | 0.954 | 0.962 | 0.981 |

**Figure 11.** Determination of A value by plotting $0.5[(1-\alpha)^{-2}-1]$ against $E_a p(x)/\beta R$ for the decomposition process of AIMOIPD at the different heating rates (β) (Stage III).

4. Conclusion

The thermal decomposition of AIMOIPD was investigated in detail by TG and DTG analyses. The kinetic parameters of decomposition were obtained by the iso-conversional and invariant methods. AIMOIPD decomposed in three stages. The rate of decomposition of third stage is slow due to high energy of activation when compared to stages I and II. The decomposition reaction is endothermic as shown by the positive values of ΔG^\ddagger and ΔH^\ddagger for all the stages, which indicates that the decomposition processes are non-spontaneous processes. The decomposition kinetic models are determined for stage I as F2 whereas for stages II and III as F3.

Acknowledgments

The authors thank Dr. Paramasivan Thirumalai Perumal and Dr. Prakasam Thirumurugan, Organic Chemistry Division, CSIR-Central Leather Research Institute, Chennai, for their fruitful suggestions and The Head, Indian Institute of Technology, SAIF, Chennai for TGA-DTG measurements.

References

- [1]. Bhaskar, G.; Arun, Y.; Balachandran, C.; Saikumar, C.; Perumal, P. T. *Eur. J. Med. Chem.* **2012**, *51*, 79-91.
- [2]. Gribble, G. W. *J. Chem. Soc. Perkin Trans. I.* **2000**, 1045-1075.
- [3]. Farghaly, A. M.; Habib, N. S.; Khalil, M. A.; El-Sayed, O. A.; *Alexandria. J. Pharm. Sci.* **1989**, *3*, 84-86.
- [4]. MacDonald, J. P.; Badillo, J. J.; Arevalo, G. E.; García, A. S.; Franz, A. K. *ACS. Comb. Sci.* **2012**, *14*, 285-293.
- [5]. Radwan, M. A. A.; Ragab, E. A.; Sabary, N. M.; Shenawy, S. M. E. *Bioorg. Med. Chem.* **2007**, *15*, 1206-1211.
- [6]. Fuchao, Y.; Huang, R.; Hangchen, N.; Juan, F.; Shengjiao, Y.; Lin, L. *Green. Chem.* **2013**, *15*, 453-462.
- [7]. Ramachary, D. B.; Chintalapudi, V.; Madhavachary, R. *Org. Lett.* **2013**, *15*, 3043-3045.
- [8]. Arun, Y.; Bhaskar, G.; Balachandran, C.; Ignacimuthu, S.; Perumal, P. T. *Bioorg. Med. Chem. Lett.* **2013**, *23*, 1839-1845.
- [9]. Maria, M. M.; Santos. *Tetrahedron*, **2014**, *70*, 9735-9757.
- [10]. Yu, B.; Yu, D. Q.; Liu, H. M. *Eur. J. Med. Chem.* **2015**, *97*, 673-698.
- [11]. Georgieva, V.; Zvezdova, D.; Vlaev, L. *Chem. Cent. J.* **2012**, *6*, 81, 1-10.

- [12]. Georgieva, V.; Zvezdova, D.; Vlaev, L. *J. Therm. Anal. Calorim.* **2013**, *111*, 763-771.
- [13]. Fulfias, A.; Vlase, G.; Vlase, T.; Soica, C.; Heghes, A.; Craina, M.; Ledeti, I. *Chem. Cent. J.* **2013**, *7*, 70, 1-9.
- [14]. Fulfias, A.; Vlase, G.; Grigorie, C.; Ledeti, I.; Albu, P.; Bilanin, M.; Vlase, T. *J. Therm. Anal. Calorim.* **2013**, *113*, 265-271.
- [15]. Kamel, T. L. *Eur. J. Chem.* **2015**, *6*(2), 199-203.
- [16]. Nalini, G.; Jayachandramani, N.; Thanikachalam, N.; Jayabharathi. J.; Manikandan, G.; Suresh, R. *Can. Chem. Trans.* **2016**, *4*, 62-76.
- [17]. Nandakumar, A.; Thirumurugan, P.; Perumal, P. T.; Vembu, P.; Ponnuswamy, M. N.; Ramesh, P. *Bioorg. Med. Chem. Lett.* **2010**, *20*, 4252-4258.
- [18]. Coats, A. W.; Redfern, J. P. *Nature (London)* **1968**, *201*, 68-69.
- [19]. Wendlandt, W. W. *Thermal Methods of Analysis*, John Wiley and Sons Inc, New York. 1974.
- [20]. Friedman, H. L. *Polym. Sci.* **1963**, *C6*, 183-195.
- [21]. Flynn, J. H.; Wall, L. A. *J. Res. Natl. Bur. Stand.* **1966**, *A70*, 487-523.
- [22]. Ozawa, T. *Bull. Chem. Soc. Jpn.* **1965**, *38*, 1881-1886.
- [23]. Kissinger, H. E. *Anal. Chem.* **1957**, *29*, 1702-1706.
- [24]. Akahira, T.; Sunose, T. *Res. Report Chiba Inst. Technol.* **1971**, *16*, 22-31.
- [25]. Malek, J. *Thermochim. Acta* **1989**, *136*, 337-346.
- [26]. Bamford, C. H.; Tipper, C. F. H. *Comprehensive chemical kinetics. Reactions in the Solid State 1980*, *22*, pp. 1-340.
- [27]. Cordes, H. F. *J. Phys. Chem.* **1968**, *72*, 2185-2189.
- [28]. Vyazovkin, S.; Linert, W. *Chem. Phys.* **1995**, *193*, 109-118.
- [29]. Budrugaec, P.; Segal, E. *J. Therm. Anal. Calorim.* **2007**, *88*, 703-707.
- [30]. Pratap, A.; Rao, T. L. S.; Dhaurandhar, H. D. *J. Therm. Anal. Calorim.* **2007**, *89*, 399-405.
- [31]. Vyazovkin S. V.; Lesnikovich, A. I. *Thermochim. Acta* **1988**, *128*, 297-300.
- [32]. Ma, H. X.; Yan, B.; Li, Z. N.; Song, J. R.; Hu, R. Z. *J. Therm. Anal. Calorim.* **2009**, *95*, 437-444.
- [33]. Boonchom, B. *J. Therm. Anal. Calorim.* **2010**, *31*, 416-429.